Responses of a Newly Evolved Auxotroph of Chlamydomonas to B_{12} Deprivation[1][CC-BY]

Freddy Bunbury,[a] Katherine E. Helliwell,[b,c] Payam Mehrshahi,[a] Matthew P. Davey,[a] Deborah L. Salmon,[c] Andre Holzer,[a] Nicholas Smirnoff,[c] and Alison G. Smith[a,2,3]

[a]Department of Plant Sciences, University of Cambridge, Downing Street, Cambridge, CB2 3EA, United Kingdom
[b]Marine Biological Association of the United Kingdom, Citadel Hill, Plymouth EX4 4PY, United Kingdom,
[c]School of Biosciences, University of Exeter, Exeter, PL1 2PB, United Kingdom

ORCID IDs: 0000-0002-2830-3674 (F.B.); 0000-0002-2068-576X (K.E.H.); 0000-0002-7192-0942 (P.M.); 0000-0002-5220-4174 (M.P.D.); 0000-0002-2575-8278 (D.L.S.); 0000-0003-2439-6364 (A.H.); 0000-0001-5630-5602 (N.S.); 0000-0001-6511-5704 (A.G.S.)

The corrinoid B_{12} is synthesized only by prokaryotes yet is widely required by eukaryotes as an enzyme cofactor. Microalgae have evolved B_{12} dependence on multiple occasions, and we previously demonstrated that experimental evolution of the non–B_{12}-requiring alga *Chlamydomonas reinhardtii* in media supplemented with B_{12} generated a B_{12}-dependent mutant (hereafter metE7). This clone provides a unique opportunity to study the physiology of a nascent B_{12} auxotroph. Our analyses demonstrate that B_{12} deprivation of metE7 disrupts C1 metabolism, causes an accumulation of starch and triacylglycerides, and leads to a decrease in photosynthetic pigments, proteins, and free amino acids. B_{12} deprivation also caused a substantial increase in reactive oxygen species, which preceded rapid cell death. Survival could be improved without compromising growth by simultaneously depriving the cells of nitrogen, suggesting a type of cross protection. Significantly, we found further improvements in survival under B_{12} limitation and an increase in B_{12} use efficiency after metE7 underwent a further period of experimental evolution, this time in coculture with a B_{12}-producing bacterium. Therefore, although an early B_{12}-dependent alga would likely be poorly adapted to coping with B_{12} deprivation, association with B_{12}-producers can ensure long-term survival whilst also providing a suitable environment for evolving mechanisms to tolerate B_{12} limitation better.

Over 50% of algal species require an exogenous source of B_{12} for growth (Croft et al., 2005), yet large areas of the ocean are depleted of this vitamin (Panzeca et al., 2009; Sañudo-Wilhelmy et al., 2012). Eukaryotic algae cannot synthesize B_{12} and must instead obtain it from certain B_{12}-producing prokaryotes (Croft et al., 2005). Indeed, while dissolved B_{12} concentrations are positively correlated with bacterioplankton density (Gobler et al., 2007; Panzeca et al., 2008), they have been found to negatively correlate with phytoplankton abundance (Ohwada, 1973; Sañudo-Wilhelmy et al., 2006). Furthermore, nutrient amendment experiments suggest that B_{12} limits phytoplankton growth in many aquatic ecosystems (Bertrand et al., 2007; Browning et al., 2017; Cohen et al., 2017). Despite this, understanding of the physiological and metabolic adaptations that B_{12}-dependent algae use to cope with B_{12} deprivation is limited.

In many algae, B_{12} is required as a cofactor for the B_{12}-dependent methionine (Met) synthase enzyme (METH; Helliwell et al., 2011), although some algae encode a B_{12}-independent isoform of this enzyme (METE) and thus do not require B_{12} for growth. Bertrand et al. (2012) showed that the B_{12}-dependent marine diatom *Thalassiosira pseudonana*, which possesses only METH, responds to B_{12} scarcity by increasing uptake capacity and altering the expression of enzymes involved in C1 metabolism. Heal et al. (2019) found that despite these responses, B_{12} deprivation disrupted the central Met cycle, transulfuration pathway, and polyamine biosynthesis. *Phaeodactylum tricornutum*, a marine diatom that uses but does not depend on B_{12} (encoding both METE and METH), responds similarly to *T. pseudonana* (Bertrand et al., 2012), but can also rely on increasing expression of METE to maintain the production of methionine. Phylogenetic analysis of the *METE* gene among diatoms shows no simple pattern of gene loss or gain, as indeed is the case across the eukaryotes (Helliwell et al., 2013;

[1]This work was supported by the Biotechnology and Biological Sciences Research Council (BBSRC) Doctoral Training Partnership (grant no. BB/M011194/1 to F.B. and A.G.S.; grant no. BB/M018180/1 to P.M. and A.G.S.; and grant no. BB/I013164/1 to K.E.H. and A.G.S.); Leverhulme Trust (grant no. RPG 2017–077 to M.P.D. and A.G.S.); Natural Environment Research Council (NERC; grant no. NE/R015449/1 to K.E.H.); and Gates Cambridge Trust (PhD scholarship to A.H.).

[2]Author for contact: as25@cam.ac.uk.
[3]Senior author.

The author responsible for distribution of materials integral to the findings presented in this article in accordance with the policy described in the Instructions for Authors (www.plantphysiol.org) is: Alison G. Smith (as25@cam.ac.uk).

F.B., P.M., and A.G.S designed the research; F.B., D.S., and A.H. performed the research and analyzed the data; M.P.D., D.S., and N.S. contributed new reagents or analytic tools; F.B., K.E.H., P.M., and A.G.S. wrote the paper with input from all authors.

www.plantphysiol.org/cgi/doi/10.1104/pp.19.01375

Ellis et al., 2017), but there is a clear link between the lack of a functional copy of the *METE* gene and B_{12} dependence (Helliwell et al., 2011; Helliwell, 2017).

As with the diatoms, the phylogenetic distribution of *METE* within the *Volvocales* (a family of green freshwater algae) points to gene loss on several independent occasions. The genomes of two volvocalean algae, *Volvox carteri* and *Gonium pectorale*, contain *METE* pseudogenes, indicating that B_{12} dependence has evolved relatively recently in these species (Helliwell et al., 2011). *Chlamydomonas reinhardtii* is a related alga that possesses a functional copy of *METE* and so is B_{12}-independent. We were able to generate a *METE* mutant of *C. reinhardtii* by experimental evolution in conditions of high vitamin B_{12} concentration over ~500 cell generations (Helliwell et al., 2015), demonstrating that sustained levels of B_{12} in the environment can drive *METE* gene loss. This mutant, which contained a Gulliver-related transposable element in the 9th exon of the *METE* gene, was completely reliant on B_{12} for growth, but in the presence of the vitamin it was able to outcompete its B_{12}-independent progenitor. In the absence of B_{12}, the *METE* mutant would sometimes revert to B_{12} independence and resume growth. Reversion was found to be due to excision of the transposon to leave behind a wild-type *METE* gene sequence, but there was a single case where a 9-bp fragment of the transposon was left behind resulting in a stable B_{12}-dependent strain, hereafter called metE7.

C. reinhardtii is a well-researched model organism that has been instrumental in improving our understanding of algal photosynthesis, ciliogenesis, and responses to fluctuating nutrient environments (Rochaix, 1995; Grossman, 2000; Dubini et al., 2009). We wanted to use the metE7 mutant of *C. reinhardtii* to study how recently acquired B_{12} auxotrophy impacts an organism's fitness and physiology, and to provide insight into the metabolic challenges that other B_{12}-dependent algae might have faced when they first evolved. In this work, we characterized the responses of metE7 to different vitamin B_{12} regimes and compared them with the responses of its ancestral B_{12}-independent strain as well as those of a closely related, naturally B_{12}-dependent alga *Lobomonas rostrata*. The responses to B_{12} deprivation were quantified by measuring changes in gene expression, cellular composition, photosynthetic activity, and viability and were contrasted against changes under nitrogen deprivation. To assess whether a recently evolved algal B_{12} auxotroph could improve its survival during B_{12} deprivation relatively quickly, we subjected metE7 to a further experimental evolution period of several months in limited B_{12} or coculture with a B_{12}-producing bacterium and characterized the resulting lines.

RESULTS

B_{12} Deprivation Causes Substantial Changes to C1 Metabolism in the metE7 Mutant

Met synthase plays a central role in the C1 cycle (Fig. 1A) and thus facilitates nucleotide synthesis and production of the universal methyl donor *S*-adenosyl-Met, which is essential for many biosynthetic and epigenetic processes (Lieber and Packer, 2002; Ducker and Rabinowitz, 2017). Wild-type *C. reinhardtii* can operate this cycle in the absence of B_{12} using the Met synthase variant METE, but metE7 relies solely on the B_{12}-requiring METH isoform. Although our main aim was to characterize the phenotype of a unique experimentally evolved B_{12}-dependent strain, metE7, we also wanted to confirm that the mutation in *METE* was solely responsible for the B_{12} dependence of this strain. We therefore generated an independent *METE* mutant line (metE4) using CRISPR/Cpf1 on a background strain suitable for genetic manipulation (UVM4; Ferenczi et al., 2017). This mutant has an in-frame stop codon resulting in a truncated METE amino acid sequence and, as predicted, exhibits B_{12} dependence (Supplemental Fig. S1). Having demonstrated the role of *METE* in providing B_{12} independence, we returned our focus to the experimentally evolved B_{12}-dependent strain, metE7, which is perhaps

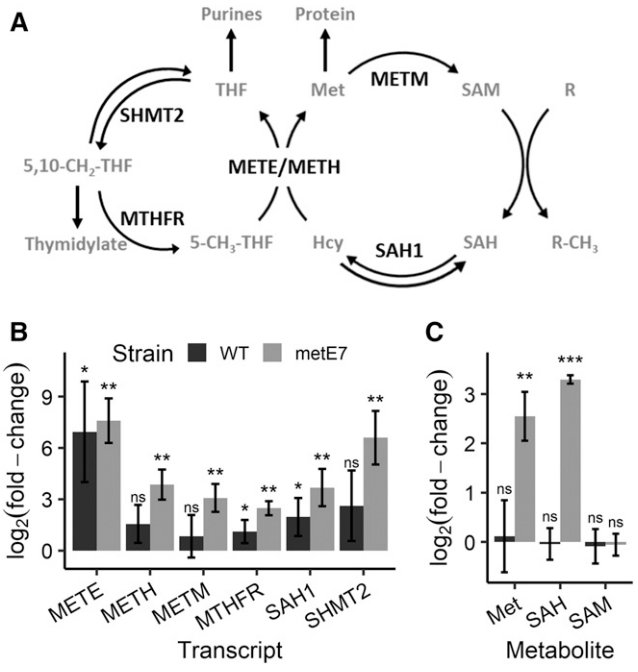

Figure 1. C1 cycle metabolites and transcripts increase during B_{12} deprivation of metE7. A, Metabolic map of a portion of the C1 cycle centered around METE and METH, with enzyme abbreviations in black, metabolite abbreviations in gray, and arrows depicting enzyme-catalyzed reactions. B, Abundances of six transcripts for enzymes of the C1 cycle measured by RT-qPCR on RNA extracted from the ancestral line and metE7 after 30 h of incubation in mixotrophic conditions with (1000 ng·L^{-1}) or without B_{12}. WT, wild type. C, Abundances of Met, SAM, and SAH metabolites measured by HPLC-MS on the same samples as above. Metabolite and transcript abundances are expressed as levels in B_{12}-deprived conditions relative to B_{12}-replete conditions and presented on a $\log_2()$ scale. Error bars = SD, $n = 3$ to 4; ns, not significant. $^*P < 0.05$, $^{**}P < 0.01$, and $^{***}P < 0.001$, Welch's t test. Wild type, ancestral B_{12}-independent strain; metE7, experimentally evolved B_{12}-dependent line. See also Supplemental Figure S2.

more reflective of B_{12}-dependent algae that have arisen naturally.

Both the wild-type ancestral line and metE7 were precultured in Tris-acetate phosphate (TAP) medium in continuous light with adequate (200 $ng \cdot L^{-1}$) B_{12} to maintain a low cellular quota of the vitamin. The cells were then pelleted, washed, and transferred to B_{12}-replete (1000 $ng \cdot L^{-1}$) or B_{12}-deprived (no B_{12}) TAP medium at 5×10^5 cells/mL and grown for 30 h. Steady-state transcript levels of six enzymes in the C1 cycle were investigated by reverse transcription-quantitative PCR (RT-qPCR; Fig. 1B). In the wild type, three transcripts (*METE*, *SAH1*, and *MTHFR*) were significantly ($P < 0.05$) upregulated by B_{12} deprivation, whereas in metE7 transcripts for all six enzymes (including *METH*, *METM*, and *SHMT2*) increased. Levels of the Met-cycle metabolites Met, SAM, and SAH were quantified by HPLC-mass spectrometry (MS). In the wild type, there was no difference in Met, SAM, or SAH levels between the two conditions (Fig. 1C). However, in metE7 cells under B_{12} deprivation, Met levels were raised 6-fold, which was somewhat unexpected given that Met synthase activity was impeded. SAH levels were also significantly elevated, whereas there was no effect on SAM. Consequently, the SAM:SAH ratio decreased by 10-fold to 3:1 under B_{12} deprivation. We then studied the dynamics of these changes by measuring metabolites and RNA abundance at several points during 3 d of B_{12} deprivation and then for 2 d following the addition of 1000 $ng \cdot L^{-1}$ B_{12}. The transcripts for all six tested C1-cycle genes increased rapidly in the first 6 h and then plateaued; reintroduction of B_{12} led to an immediate reduction to near initial amounts (Supplemental Fig. S2A). Similar profiles were seen for the metabolites SAM and SAH, although the peak occurred later at 24 h (Supplemental Fig. S2B). Met levels were more variable, but nonetheless there was a similar trend of a peak 24 h after removal of B_{12}. More significantly, the SAM:SAH ratio fell sharply from 30 to less than 1 within 24 h. A subsequent gradual increase occurred over the next 2 d, and resupply of B_{12} increased this ratio further over the following 2 d. The likelihood therefore is that many cellular processes would be impacted in B_{12}-deprived metE7 cells.

B_{12} Deprivation Significantly Impacts Cell Physiology and Biochemical Composition

Our data demonstrated a substantial impact of B_{12} limitation on the expression of C1 metabolic genes as well as the abundance of C1 metabolites. To elucidate downstream consequences of perturbed C1 metabolism, we also characterized broader physiological responses to B_{12} deprivation. As has been documented previously (Helliwell et al., 2015), growth of metE7 cells was significantly impaired in B_{12}-deprived conditions (Supplemental Fig. S3A). However, by day 2 the B_{12}-deprived cells had a 36% larger diameter resulting in a 150% increase in volume (Fig. 2A; Supplemental Fig. S3B), indicating that cell division was more restricted than overall growth. Moreover, cell viability, which was assayed by the ability of cells to form colonies when plated on B_{12}-replete TAP agar, decreased to below 25% within 4 d of B_{12} limitation (Supplemental Fig. S3C). This was preceded by a reduction in PSII maximum efficiency (*Fv/Fm*; Supplemental Fig. S3D), an often-used indicator of algal stress (Parkhill et al., 2001; White et al., 2011).

The biochemical composition of *C. reinhardtii* cells is altered considerably and similarly under various nutrient deprivations; therefore, we hypothesized that B_{12} limitation would also induce broadly the same responses (Grossman, 2000; Juergens et al., 2016; S. Saroussi et al., 2017). Therefore, metE7 cells were precultured as before in 200 $ng \cdot L^{-1}$ B_{12} and then washed and resuspended in TAP with or without B_{12} (1000 $ng \cdot L^{-1}$) and cultured mixotrophically for 4 d. Cultures were visually inspected by microscopy (Fig. 2A), and the amounts of various cellular components were measured on days 2 and 4 (Fig. 2B; Supplemental Fig. S4). Chlorophyll levels declined considerably under B_{12} deprivation so that by day 4 the cells had a bleached appearance with an 85% lower concentration than the B_{12}-replete cells. Similarly, free fatty acids, polar lipids, and proteins were at least 50% lower under B_{12}-deprivation conditions on day 4. Starch content, on the other hand, showed the largest

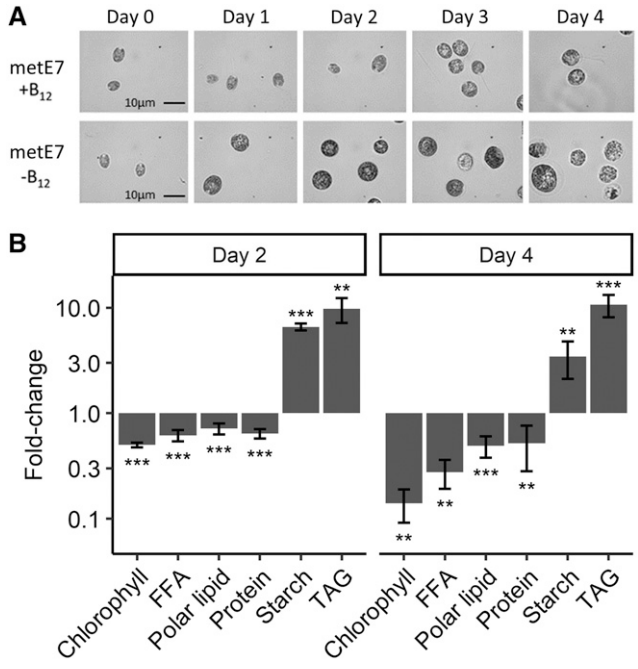

Figure 2. B_{12} deprivation of metE7 causes cell enlargement and significant changes in biochemical composition. A, Micrographs taken at 1000× magnification of metE7 cells grown in TAP medium with (1000 $ng \cdot L^{-1}$) or without B_{12} over a period of 4 d. B, Biochemical composition of B_{12}-deprived cells on days 2 and 4 of the growth period expressed as mass of those compounds normalized to total cell dry mass and then expressed relative to the amounts in B_{12} replete conditions. Error bars = SD, $n = 5$. $^{**}P < 0.01$ and $^{***}P < 0.001$, Welch's *t* test. FFA, free fatty acids. See also Supplemental Figures S3–S5.

absolute increase from B_{12}-replete to B_{12}-deprived cells (Supplemental Fig. S4), and triacylglycerides (TAG) were 10-fold higher in B_{12}-deprived cells (Fig. 2B), which effectively balanced the loss of polar lipids and free fatty acids so that overall lipid levels were roughly 8% to 10% of dry mass in both treatments. To look in more detail, quantification of free amino acids and fatty acid composition of all lipid classes was carried out (Supplemental Fig. S5). By day 4, most of the amino acids decreased significantly under B_{12} deprivation. Particularly noteworthy are the reduction in Met, in contrast with its elevation at an earlier time point, and the increase in Gln, the only amino acid that is more abundant in B_{12}-deprived cells (Supplemental Fig. S5A). Overall the degree of fatty acid saturation was higher under B_{12} deprivation, due mainly to an increase in the dominant saturated fatty acids palmitate (16:0) and stearate (18:0: Supplemental Fig. S5B), although levels of several unsaturated fatty acids, in particular 16:2, 16:3$^{(7,10,13)}$, 18:1, and 18:2, were also elevated.

Responses to Nitrogen Deprivation Improve Survival under B_{12} deprivation

B_{12} deprivation of metE7 causes several changes in biochemical composition, including accumulation of TAG and starch and decreases in chlorophyll and protein, akin to those exhibited following nitrogen deprivation of wild-type *C. reinhardtii* (Cakmak et al., 2012; Park et al., 2015; Yang et al., 2015). To investigate this comparison further we measured growth, viability, and photosynthetic efficiency under both conditions over a time course (Supplemental Fig. S6). metE7 culture density increased more under B_{12} than nitrogen deprivation (Supplemental Fig. S6A), but started to decline after day 2, unlike under nitrogen deprivation where growth continued more slowly over 4 d. For cell viability, both conditions caused a decline, but whereas loss of viability continued in B_{12}-deprived cells, under nitrogen deprivation the initial loss was followed by recovery (Supplemental Fig. S6B). Maximum photosynthetic efficiency of PSII, however, did not recover under either condition, and its decline was more rapid in nitrogen-deprived cells (Supplemental Fig. S6C).

The increased viability of metE7 under nitrogen deprivation compared with under B_{12} deprivation suggested that either the metabolic role of B_{12} would make it intrinsically more difficult to cope without or that the evolutionary naivety of metE7 to B_{12} dependence would mean it had little time to evolve protective responses to B_{12} limitation. We therefore tested whether responses to nitrogen deprivation could afford some protection against B_{12} deprivation. Viability measurements were monitored over several days, and cultures lacking either nitrogen or B_{12} behaved as previously (Fig. 3A). However, metE7 cells deprived of both nitrogen and B_{12} simultaneously were more like those starved of nitrogen, with an initial decrease in viability followed by recovery to a level significantly higher than in B_{12} deprivation alone. As total growth under B_{12}- and nitrogen-deprivation conditions was not significantly different from that under B_{12} deprivation alone (Supplemental Fig. S7), this apparent protective mechanism in response to nitrogen deprivation is not simply a result of inhibiting growth and hence avoiding severe B_{12} starvation. Instead, it seems likely that nitrogen deprivation would have elicited photoprotective responses, such as increasing nonphotochemical quenching in order to avoid the accumulation of damaging reactive oxygen species (ROS; Erickson et al., 2015; Saroussi et al., 2016; Saroussi et al., 2017, 2019), initiated the quiescence cycle to mitigate the genomic damage caused by ROS (Takeuchi and Benning, 2019), or activated the gametic survival program (Martin and Goodenough, 1975).

To investigate whether the cell death observed under B_{12} deprivation of metE7 could be due to ROS, the general ROS-sensitive dye dihydrodichlorofluorescein diacetate was incubated with cells at different time points during nutrient deprivation. We found that ROS levels increased under all nutrient-deprived conditions in the first 2 d but were highest in those cells deprived of

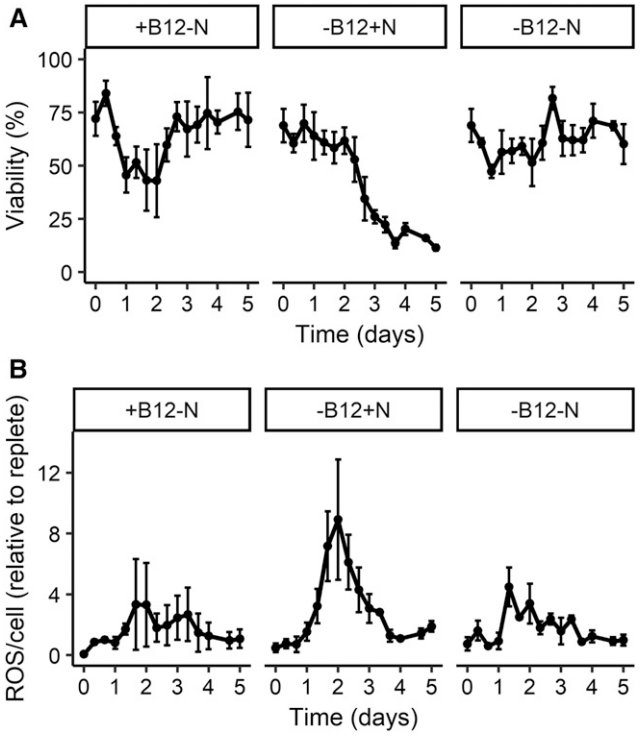

Figure 3. metE7 survives better and produces lower levels of ROS when limited for both N and B_{12} than just B_{12} alone. A, Percentage of cells that could form colonies (a measure of viability) on nutrient replete agar when removed at different time points from various nutrient deprivation conditions (indicated in panels above the graphs as follows: $+B_{12}$-N, 1000 ng·L^{-1} B_{12} and 0 mM NH_4Cl; -B_{12}+N, 0 ng·L^{-1} B_{12} and 7.5 mM NH_4Cl; or -B_{12}-N, 0 ng·L^{-1} B12 and 0 mM NH_4Cl. B, ROS measured by dichlorofluorescein diacetate fluorescence and normalized both on a per cell basis and to the nutrient replete treatment ($+B_{12}$+N). Error bars = SD, n = 3 to 6. See also Supplemental Figures S6 and S7.

B_{12} alone (Fig. 3B). This peak coincided with the start of the substantial decline in cell viability (Fig. 3A). The combination of B_{12} and nitrogen deprivation reduced ROS levels to similar amounts to those seen in the nitrogen-deprived cells, and therefore may be a factor behind reduced cell death.

Natural B_{12} Auxotroph Lobomonas rostrata Fares Better under B_{12}-Limiting Conditions than metE7

Considering that metE7 quickly lost viability in the absence of B_{12} while nitrogen starvation invoked protective responses independent of B_{12} status, it is possible that as a novel auxotroph, the response of metE7 to B_{12} deprivation is simply underdeveloped. To test this, we compared the B_{12} physiology of metE7 with *L. rostrata*, a naturally B_{12}-dependent member of the same Volvocaceae family of chlorophyte algae (Provasoli, 1958; Sausen et al., 2018). Cell viability was significantly greater in *L. rostrata* cells compared with the metE7 line after 2–4 d of B_{12} deprivation despite also growing to a greater density (Supplemental Fig. S8). Moreover, a B_{12} dose-response experiment, in which the two species were each cultured mixotrophically in a range of B_{12} concentrations, revealed that *L. rostrata* reached a higher optical density than metE7 at all B_{12} concentrations below 90 $ng \cdot L^{-1}$, whereas the inverse was true above 90 $ng \cdot L^{-1}$ (Fig. 4A). This indicates that *L. rostrata* has a lower B_{12} requirement than metE7.

In the natural environment the ultimate source of B_{12} is from prokaryotes since they are the only known B_{12} producers (Warren et al., 2002). In separate studies it was shown that B_{12}-dependent growth of *L. rostrata* and metE7 can be supported by the B_{12}-synthesizing bacterium *Mesorhizobium loti* (Kazamia et al., 2012; Helliwell et al., 2015). We therefore directly compared the growth of metE7 and *L. rostrata* in B_{12}-supplemented (100 $ng \cdot L^{-1}$) axenic culture and in coculture with *M. loti* in media lacking a carbon source (TP; Fig. 4A). Even though metE7 grew much more quickly and to a higher density than *L. rostrata* under axenic, B_{12}-supplemented conditions, it grew less well in coculture with *M. loti* (Fig. 4B), indicating that B_{12} provision from the bacterium is less effective at supporting the growth of metE7 than of *L. rostrata*. This may simply be due to their different B_{12} requirements, or to more sophisticated symbiotic interactions.

Experimental Evolution in Coculture Improves B_{12} Use Efficiency and Resilience to B_{12} Deprivation

Together, our data suggest that the newly evolved metE7 line is poorly adapted to coping with B_{12} deprivation, but we wanted to determine whether the metE7 line could evolve improved tolerance to B_{12} limiting conditions, so we used an experimental evolution approach (Supplemental Fig. S9). We designed three distinct conditions, referred to as H, L, and C. Condition H

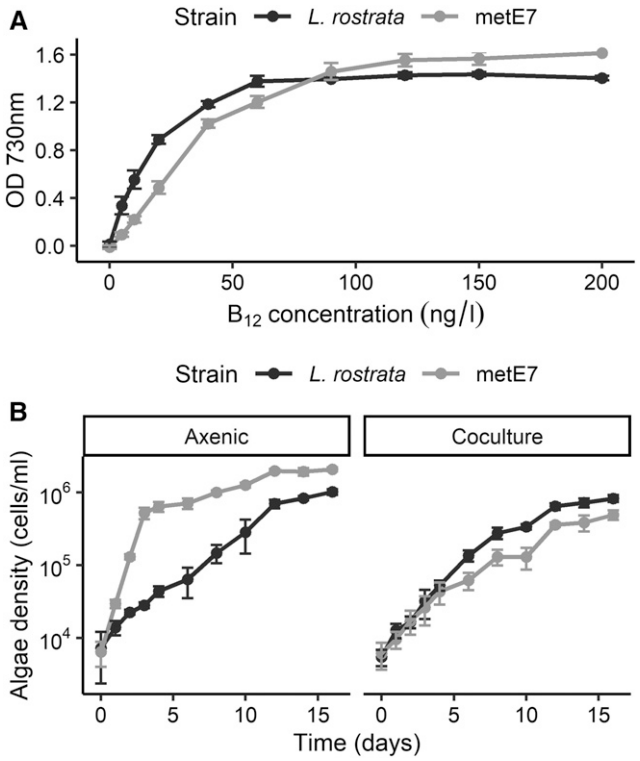

Figure 4. *L. rostrata* grows better than metE7 in coculture with a B_{12}-producing bacterium, in part due to its lower demand for B_{12}. A, Precultures of the algae, grown with 200 $ng \cdot L^{-1}$ B_{12}, were washed and inoculated at roughly 100 $cells \cdot mL^{-1}$ and then grown mixotrophically (TAP medium in continuous light), with B_{12} concentrations from 0 to 200 $ng \cdot L^{-1}$. OD at 730 nm was measured after 5 and 9 d of growth for metE7 and *L. rostrata*, respectively. B, Cultures were grown photoautotrophically (TP media in 16-h light [100 $\mu E \cdot m^{-2} \cdot s^{-1}$]:8-h dark cycles) in axenic culture (with 100 $ng \cdot L^{-1}$ B_{12}) or coculture (with the B_{12}-producing bacterium *M. loti*) over a period of 16 d with cell density measurements performed every 1 to 2 d. For both (A) and (B), black = *L. rostrata*, gray = metE7, error bars = SD, $n = 4$. See also Supplemental Figure S8.

(TAP medium with high [1000 $ng \cdot L^{-1}$] B_{12}) was a continuation of the conditions that had initially generated metE7 (Helliwell et al., 2015). Condition L (TAP medium with low [25 $ng \cdot L^{-1}$] B_{12}) was chosen so that B_{12} would limit growth. Condition C (coculture with *M. loti* in TP medium) was a simplification of an environmental microbial community. Eight independent cultures for each condition were established from a single colony and then subcultured once per week over a total period of 10 months (~1000 cell generations). To account for the different growth rates in the three conditions, we applied the dilution rates of 10,000, 100, and 5 times per week in condition H, L, and C, respectively (Supplemental Fig. S9). After 10 months under selective conditions, all 24 cultures had survived and were then treated with antibiotics to remove the *M. loti* from condition C and to ensure that there were no other contaminating bacteria. We then subcultured all 24 evolved lines alongside eight replicates of the progenitor

strain (which had been maintained on TP agar with 1000 ng·L^{-1} B_{12} without subculturing) in mixotrophic conditions with TAP + 200 ng·L^{-1} B_{12} three times over 9 d to ensure they were all acclimated to the same conditions. The behaviors of the algal populations, hereafter referred to as metE7, metE7H, metE7L, and metE7C, were then compared with one another for their responses to different B_{12} concentrations, B_{12} deprivation, and growth in coculture with the B_{12}-producer *M. loti*.

Under high levels of B_{12} (>320 ng·L^{-1}), a similar carrying capacity was reached by the progenitor metE7 strain and the metE7H and metE7C populations, whereas metE7L density was significantly lower than the progenitor (Supplemental Fig. S10A). When grown across a range of B_{12} concentrations to determine a dose response, the metE7C populations reached a significantly higher optical density at the lower concentrations of 20 and 40 ng·L^{-1} B_{12} than the other lines (Fig. 5A). The concentration of B_{12} required to produce half the maximum growth (EC_{50}) of metE7C was therefore much lower than the progenitor metE7 or metE7H (Supplemental Fig. S10B) and this was reflected in the higher B_{12} use efficiency, i.e. the maximal increase in yield (optical density $[OD]_{730}$) that results from an increase in B_{12} concentration (Fig. 5B). However, the maximal growth rate of metE7C was significantly lower (Supplemental Fig. S10C), and it is tempting to conclude that this is a necessary trade-off. We also compared the viability of the experimentally evolved lines during B_{12} deprivation (Fig. 5C). Figure 5C shows that although all lines lost viability during B_{12} deprivation, metE7L and metE7C survived substantially better, with a median survival time more than a day longer (Fig. 5D) than both the progenitor metE7 and metE7H. Finally, we compared the growth of the evolved lines in coculture with *M. loti*, which showed, perhaps unsurprisingly, that the metE7C lines grew better than the others (Fig. 5E), and at the end of the growth period had a significantly higher number of algae supported per bacterium (Fig. 5F).

To elucidate which factors contributed to improved survival during B_{12} deprivation, we performed

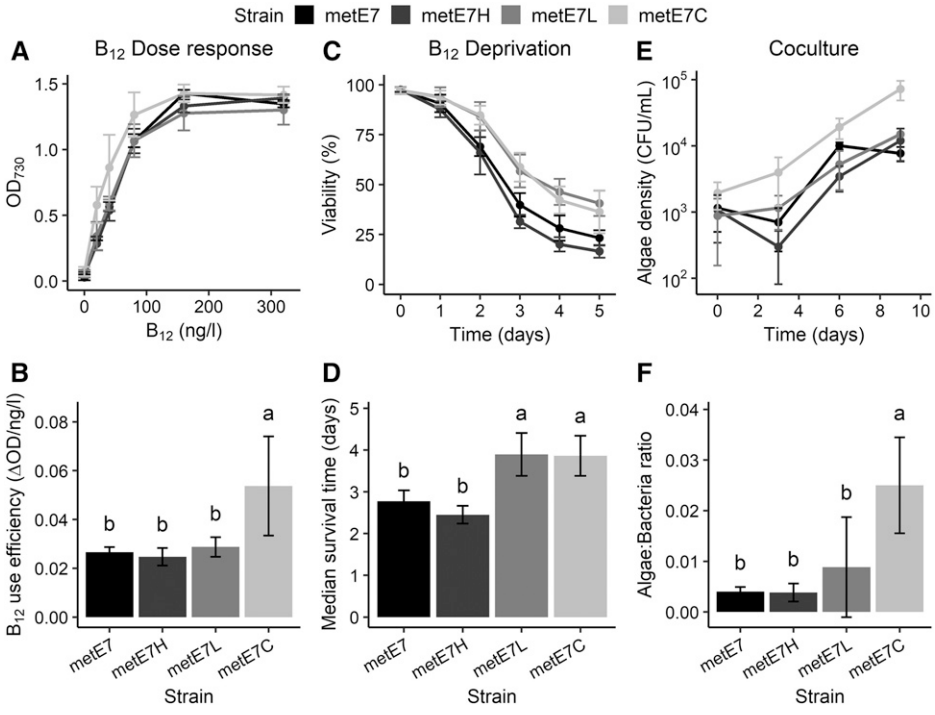

Figure 5. Experimental coevolution of metE7 with the bacterium *M. loti* selects for improved algal growth in coculture, increased B_{12} use efficiency, and better resilience to B_{12} deprivation. A, Maximum optical density achieved by mixotrophically grown cultures of experimentally evolved lines of metE7 grown over a period of 12 d in six different concentrations of B_{12}. B, B_{12} use efficiency of evolved lines calculated using a fitted Monod equation and expressed as the maximum rate of increase in OD_{730} that would result from an increase in B_{12} concentration. C, Viability (measured as the percentage of cells capable of forming colonies on B_{12}-replete agar) of mixotrophically grown cultures of experimentally evolved lines of metE7 over a 5-d period cultured in 40 ng· l^{-1} B_{12}. D, Median survival time of evolved lines after dilution of culture to 40 ng· L^{-1} B_{12} calculated using a fitted Verhulst equation. E, Algal cell density of photoautotrophically grown cocultures of experimentally evolved lines of metE7 with *M. loti* over a 9-d period. F, Ratio of algae to bacteria on the final day (day 9) of growth in coculture. metE7H = metE7 evolved in TAP + 1,000 ng· L^{-1} B_{12} for 10 months; metE7L = metE7 evolved in TAP media + 25 ng· L^{-1} B_{12}; metE7C = metE7 evolved in Tris minimal medium in coculture with the B_{12}-producing bacterium *M. loti*. Mean of 7 to 8 independently evolved lines are shown. Error bars = 95% confidence interval. Letters above error bars indicate statistical groupings provided by Tukey's range test, which was performed following a significant ANOVA result. See also Supplemental Figures S9 and S10.

a multivariable physiological analysis (Fig. 6). Sixteen variables or parameters were measured across the 32 metE7 populations and the dataset (Supplemental Dataset) was visualized in two ways. Figure 6A displays the first two components of a principal component analysis of the data, which confirmed that the experimental evolution populations tended toward forming separate clusters, with the metE7C populations most diverged from the progenitor metE7, due mainly to higher B_{12} use efficiency and median survival time, but lower maximal growth rate, carrying capacity, and EC_{50} for B_{12}. Figure 6B is a correlation matrix of the parameters, which reveals those pairs that are most positively or negatively correlated with one another. For example, median survival time was quite highly negatively correlated with maximal growth rate and positively correlated with B_{12} use efficiency.

A more definitive statistical approach was then used to determine the most important measurements for predicting survival time during B_{12} deprivation: using stepwise minimization of the Bayesian information criterion of the full additive linear model, the 15 other measurements (all 16 minus median survival time) were reduced to just three. These three measurements, higher B_{12} use efficiency, lower ROS levels, and lower maximal growth rate, can therefore be considered sufficient to explain longer survival time under B_{12} deprivation of the metE7 populations. Using the same method, we also investigated which values best predicted growth in coculture with *M. loti*, using algae:bacteria ratio as a proxy for this. We found that algae:bacteria ratio was also optimally predicted by just three measurements: higher algal B_{12} use efficiency and lower algal maximal growth rate, as for survival time, but also lower algal B_{12} uptake capacity. Together these results indicate that experimental evolution in coculture not only improves growth in coculture but also increases B_{12} use efficiency and survival during B_{12} deprivation.

DISCUSSION

In this study, we exploited a new model system for the evolution of vitamin B_{12} dependence by analyzing the physiological and metabolic responses to B_{12} deprivation of an artificially evolved B_{12}-dependent mutant

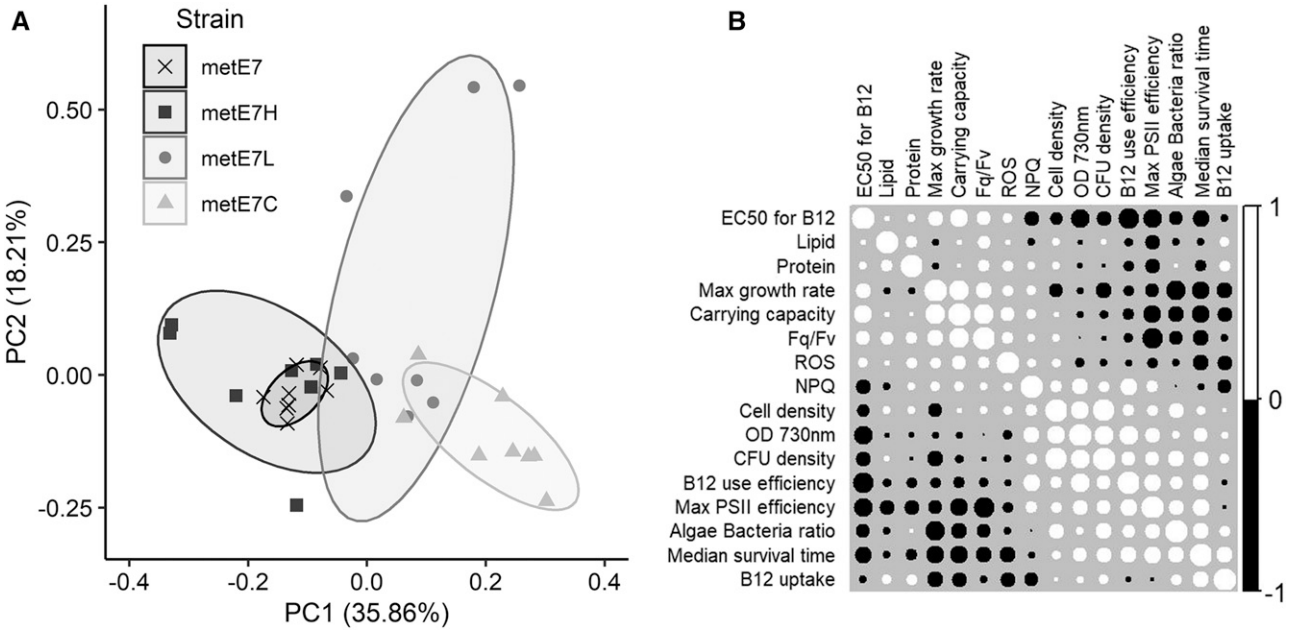

Figure 6. Analysis of a range of measurements made or parameters calculated from the metE7 progenitor strain and its experimental evolution descendants. A, Plot of the first two principal components derived from principal component analysis applied to these measured variables and calculated parameters. Each point represents an evolved line or replicate of the progenitor strain and is given a color and shape according to experimental evolution condition, which is specified in the key in the top left corner. Ellipses are created to show the SD of the eight lines belonging to these experimental evolution groups. B, Correlation matrix of all the measured parameters in which white circles represent positive correlation, black circles represent negative correlation, and the size of the circle represents the magnitude of the R^2 value. B_{12} use efficiency, carrying capacity, EC_{50} for B_{12}, and max growth rate were calculated using all time points from the B_{12} dose response experiment (Fig. 5A). Median survival time was calculated using all measurements of viability during B_{12} deprivation (Fig. 5C). Algae:Bacteria ratio was taken from the final day (day 9) of coculturing the strains with the bacterium *M. loti* (Fig. 5E). All other variables (B_{12} uptake [$_{12}$ absorbed in 1 h per unit OD], max PSII efficiency [*Fv/Fm*], CFU density [colony forming units per milliliter], OD 730 nm [OD of cultures at 730 nm], cell density [total cells per milliliter], NPQ [nonphotochemical quenching], ROS [ROS per unit OD], Fq/Fv [coefficient of photochemical quenching], protein [protein concentration per unit OD], and lipid [lipid concentration per unit OD]) were the averages of all available measurements taken during B_{12} deprivation.

of *C. reinhardtii*. Our analyses demonstrate that B_{12} deprivation has important consequences for C1 metabolism: we observed a significant increase in the transcript abundance of C1-cycle enzymes in both the wild type and metE7 strain, and a decrease in the methylation index (SAM:SAH ratio) in metE7 only. Moreover, B_{12} deprivation of metE7 causes a decrease in chlorophyll, protein, and amino acids, and an increase in starch, lipids, and saturated fatty acids, characteristic of limitation responses to macronutrients such as nitrogen (Cakmak et al., 2012; Yang et al., 2015; Park et al., 2015; Juergens et al., 2016). The rapid loss of viability seen under B_{12} deprivation could be averted if the metE7 cells were also limited for nitrogen, suggesting that it is not the lack of B_{12} per se that causes cell death, but an inability to respond appropriately. Together this suggests a newly evolved B_{12} auxotroph would be poorly adapted to surviving in the natural environment where a B_{12} supply is not guaranteed. However, we found that metE7 can be supported for several months by a B_{12}-producing bacterium, and experimental evolution under these conditions caused improved B_{12} use efficiency and resilience to B_{12} deprivation.

B_{12} deprivation of metE7 decreased the SAM:SAH ratio 10-fold, mainly due to an accumulation of SAH, reflecting a recent B_{12} deprivation study of the diatom *T. pseudonana* (Heal et al., 2019), numerous observational studies of B_{12} deficiency in humans (Guerra-Shinohara et al., 2004; Stabler et al., 2006), and studies of disrupted C1 metabolism in Arabidopsis (Meï et al., 2017). As SAH is a competitive inhibitor of methyltransferases (Chiang et al., 1996), this decrease would likely lead to general hypomethylation in metE7. The epigenetic marks methyldeoxyadenosine and methylcytosine are similarly abundant in *C. reinhardtii* and appear to mark active genes and repeat-rich regions, respectively; therefore, the consequences of hypomethylation are unclear (Fu et al., 2015; Lopez et al., 2015). The reduced abundance of B_{12}-bound METH under B_{12} deprivation would hinder Met synthesis and could cause the observed reduction in protein abundance (Fig. 2B). However, Met levels increased between 12 and 24 h of B_{12} deprivation (Supplemental Fig. S2B), suggesting a reduction in its use, proteolysis, or increased synthesis due to higher METH expression or via alternative pathways such as the *S*-methyl-Met cycle, which is known to play an important regulatory role in plants (Ranocha et al., 2001).

METE transcript abundance showed a much higher dynamic range than *METH* during B_{12} deprivation and reintroduction (Supplemental Fig. S2A), which is reflected by the higher diurnal range of *METE* observed in global transcriptomics and proteomics datasets (Strenkert et al., 2019). However, on average METE is ~60-fold more abundant than METH in *C. reinhardtii* (Strenkert et al., 2019). This may be due to a lower maximal catalytic rate of METE, as has been observed in *E. coli* (González et al, 1992), or due to its role in the flagella, which contain METE but not METH (Schneider et al., 2008). Under B_{12}-deprivation conditions, the activity of METH would be compromised, yet in both metE7 and the ancestral strains, it was upregulated. This is more similar to the B_{12}-dependent algae *T. pseudonana* and *Tisochrysis lutea*, which also up-regulate *METH* under B_{12} deprivation (Bertrand et al., 2012; Nef et al., 2019), than the B_{12}-independent *P. tricornutum*, which decreases *METH* expression (Bertrand et al., 2013). However, in both *T. pseudonana* and *P. tricornutum*, B_{12} deprivation substantially upregulates C1-cycle enzymes including homologs of *METM*, *MTHFR*, and *SAH1* (Bertrand et al., 2012), reflecting our findings here and in *L. rostrata* (Helliwell et al. 2014). Under sulfur- and nitrogen-deprivation conditions, these C1-cycle genes are down-regulated (González-Ballester et al., 2010; Schmollinger et al., 2014), suggesting that their upregulation during B_{12} deprivation is not a general response to nutrient stress, but a nutrient-specific one, as indeed is the case for *T. lutea* (Nef et al., 2019).

Chlorosis is a common symptom of nutrient deficiency in *C. reinhardtii*, evident in nitrogen-, sulfur-, iron-, and zinc-limiting conditions; therefore, it is not surprising that B_{12} deprivation of metE7 caused a substantial decline in total chlorophyll (Fig. 2B; Kropat et al., 2011; Schmollinger et al., 2014; Juergens et al., 2015). The decrease in total protein content occurred more slowly and was less substantial (50% reduction over 4 d) than that reported under nitrogen and sulfur deprivation (80% reduction within 1 d; Cakmak et al., 2012). During nitrogen and iron starvation in *C. reinhardtii*, membrane lipids decrease drastically concomitant with the increase in TAGs (Siaut et al., 2011; Urzica et al., 2013). This is very much like what we observed for metE7 under B_{12} deprivation, although here the level of free fatty acids and polar lipids decreased by a roughly similar amount to the increase in TAGs indicating there is little, if any, de novo fatty acid synthesis. In addition, B_{12} deprivation causes similar shifts in fatty acid composition to nitrogen and iron deprivation, most notably a substantial increase in palmitic acid (16:0) and decrease in polyunsaturated 16:4 fatty acid (Msanne et al., 2012; Urzica et al., 2013). Despite these similarities, B_{12} deprivation may elicit an increase in TAGs by a different pathway due to disrupted C1 metabolism, as has been observed in several organisms (da Silva et al., 2014; Meï et al., 2017; Visram et al., 2018). This is thought to be due to a reduction in the methylation potential limiting membrane lipid synthesis and hence diverting more lipids toward TAGs (Malanovic et al., 2008; Visram et al., 2018). Therefore, B_{12} deprivation could provide a complementary approach to other nutrient deprivation experiments in improving our understanding of lipid metabolism in *C. reinhardtii* and other algae.

From an evolutionary perspective, the prevalence of vitamin B_{12} dependence among algae appears somewhat at odds with the severe fitness penalties that would be incurred were they exposed to limiting dissolved B_{12} concentrations. This is made more surprising by the fact that the fitness benefit of B_{12} dependence under laboratory conditions in replete B_{12}, although

statistically significant, is relatively minimal (Helliwell et al., 2015). However, compared to the optimal axenic laboratory conditions in which the metE7 line evolved, in the natural environment multiple nutrients may colimit growth, perhaps even eliciting responses that mitigate against B_{12} deprivation, as we observed here, and B_{12}-producing bacteria may not simply co-occur with algae but also actively engage in mutualistic interactions (Croft et al., 2005; Kazamia et al., 2012, 2016; Cooper et al., 2019). Furthermore, our evidence suggests that selection under coculture conditions led to the newly evolved B_{12} auxotroph developing increased B_{12} use efficiency and becoming better adapted to tolerating B_{12} limitation, which could make this line more robust to the unreliable B_{12} supply in the natural environment. However, these improvements appeared to come at the expense of maximal growth rate in B_{12}-replete conditions (Supplemental Fig. S10C), which is not unexpected in light of previous experimental evolution studies in *C. reinhardtii* (Collins and Bell, 2004). As one of the conserved responses of *C. reinhardtii* upon detecting depletion of various nutrients is to decrease cell division, it is possible that slower growth might even be selected for under B_{12} deprivation. Indeed, a low growth rate was found to be a significant predictor of greater survival time under B_{12} deprivation, alongside low ROS levels and high B_{12} use efficiency.

The fact that metE7 survived a 10-month period either with limited artificial supplementation of B_{12} or by relying completely on bacterial B_{12} provision does suggest that even a newly evolved and poorly adapted B_{12} auxotroph would have ample opportunity to adapt further. What adaptations are likely to improve growth and survival under B_{12} deprivation are not altogether clear, but it is not unreasonable to assume that exaptation of existing nutrient limitation responses would play a major role. B_{12} dependence is certainly a risky evolutionary strategy, and one which may have ended in extinction countless times, but our work suggests that even the simplest of symbioses with B_{12}-producing bacteria may be sufficient to ensure the survival and drive the continued evolution of B_{12}-dependent algae.

MATERIALS AND METHODS

Strains

Mesorhizobium loti (MAFF 303099) was a gift from Allan Downie at the John Innes Centre. Algal strains used in this study are shown in Supplemental Table S1 and include *Lobomonas rostrata* (SAG 45/2), as well as several *Chlamydomonas reinhardtii* strains derived from strain 12 of wild-type 137c or the cell wall-deficient strain cw15. The stable B_{12}-dependent metE7 and the unstable B_{12}-dependent (S-type) as well as the B_{12}-independent revertant line (R-type) all evolved from the strain 12 of wild-type 137c (Ancestral) as described by Helliwell et al. (2015). Another B_{12}-dependent mutant (metE4) was generated by targeted (CRISPR/Cpf1) knockout of the *METE* gene in the UVM4 strain using the protocol described in Ferenczi et al. (2017). The guide RNA and single-stranded donor oligonucleotide used for homology- directed repair are given in Supplemental Table S2, alongside sequencing primers used to confirm that the modification resulted in a premature stop codon producing an 89 amino-acid protein rather than the full-length sequence of 815 amino acids sequence.

Culture Conditions and Growth Measurements

Algal colonies were maintained quarterly on TAP (Supplemental Table S5) + 1000 $ng \cdot L^{-1}$ cyanocobalamin (B_{12}) agar (1.5% [w/v]) in sealed transparent plastic tubes at room temperature and ambient light. Cultures were grown in TAP or Tris min medium under continuous light or a light-dark period of 16-h light:8-h dark cycle, at 100 $\mu E \cdot m^{-2} \cdot s^{-1}$, at a temperature of 25°C, with rotational shaking at 120 rpm in an incubator (InforsHTMultitron). For nutrient starvation experiments the preculture TAP medium contained 200 $ng \cdot L^{-1}$ of B_{12}, and when cell densities surpassed 10^6 cells $\cdot mL^{-1}$ or an OD730 nm of 0.2, cultures were centrifuged at 2,000 *g* for 2 min, followed by supernatant removal and resuspension of the cell pellet in media. For nitrogen deprivation, ammonium chloride was omitted from the media with no replacement.

Algal cell density and optical density at 730 nm were measured using a Z2 particle count analyzer (Beckman Coulter) with limits of 2.974 to 9.001 μm, and a FluoStar Optima (BMG labtech) or Thermo Spectronic UV1 spectrophotometer (ThermoFisher), respectively. Mean cell diameter was also quantified on a Z2 particle analyzer (Beckman Coulter). Dry mass was measured by filtering 20 mL of culture through predried and weighed grade-5 Whatmann filter paper (Sigma-Aldrich WHA1005090), drying at 70°C for 24 h, followed by further weighing on a Secura mass balance (Sartorius). Algal and bacterial viable cell density were determined by plating serial dilutions on solid media and counting colonies to calculate colony-forming units per milliliter (CFU $\cdot mL^{-1}$).

Measurement of Photosynthetic Parameters

Then 200 μL of cultures with an OD730 nm > 0.1 were transferred to a 96-well plate, which was then incubated at 25°C in the dark for 20 min. F_0 was measured before, and F_m during, a saturating pulse at 6172 $\mu E \cdot m^{-2} \cdot s^{-1}$. The light intensity was increased to 100 $\mu E \cdot m^{-2} \cdot s^{-1}$ and the cells allowed to acclimate for 30 s before another set of fluorescence measurements before and during a saturating pulse. From these fluorescence measurements, the CF imager software calculated nonphotochemical quenching (*Fm/Fm'-1*), PSII maximum efficiency (*Fv'/Fm'*), and the coefficient of photochemical quenching (*Fq'/Fv'*).

Measurement of Cellular Biochemical Composition

Lipids were extracted from the cell pellet from 10 mL of culture using the chloroform/methanol/water method, and TAGs, polar lipids, and free fatty acids in the total lipid extract and total fatty acid methyl esters were analyzed by gas chromatography-FID and gas chromatography-MS, as described in Supplemental Materials and Methods and Davey et al. (2014). A 1-mL aliquot of algal culture was used for pigment and starch quantification as described in Davey et al. (2014), and a 10-mL aliquot for protein quantification using a Bradford assay and amino acids by HPLC as described in Supplemental Materials and Methods and Helliwell et al. (2018).

Reactive Oxygen Species Quantification

Next, 2 μL of 1 mM 2′,7′ dichlorofluorescein diacetate (Sigma-Aldrich) dissolved in dimethyl sulfoxide was added to 198 μL of cell culture in a black f-bottom 96-well plate (Greiner bio-one) and incubated at room temperature in the dark for 60 min before recording fluorescence at 520 nm after excitation at 485 nm in a FluoStar Optima Spectrophotometer (BMG labtech). Fresh cell culture media devoid of any cells was used as a blank.

Vitamin B_{12} Quantification

A 1-mL aliquot of the culture to be tested was boiled for 5 min to release B_{12} into solution, and then the growth response of a B_{12}-dependent strain of *Salmonella typhimurium* (AR3612) incubated for 16 h at 37°C in 50% (v/v) 2*M9 media + 50% (v/v) boiled extract was quantified by measuring optical density at 600 nm. B_{12} concentration was calculated by comparing OD600 nm to a standard curve of known B_{12} concentrations using a fitted logistic model. To calculate B_{12} uptake by algal cells, B_{12} was added to an aliquot of algal culture to a concentration of 1000 $ng \cdot L^{-1}$, followed by incubation for 1 h under previously described growth conditions, then measuring the B_{12} remaining in the media (supernatant of the centrifuged aliquot). B_{12} uptake (Initial B_{12} – remaining B_{12}) was divided by OD730 nm of the aliquot to give B_{12} uptake capacity in $ng \cdot L^{-1} \cdot OD730\ nm^{-1}$.

SAM and SAH Quantification

Then, 10 mL of samples were centrifuged at 2,000 *g* for 2 min, supernatant removed, and cell pellet lyophilized at < -40°C and <10 Pa for 12–24 h. Next, 300 μL of 10% (v/v) methanol (liquid chromatography-MS grade) spiked with stable isotope-labeled amino acids (L-amino acid mix; Sigma-Aldrich) was added to each sample. They were vortexed 3 times, every 10 min, before sonicating for 15 min in an iced water bath and then centrifuging (16,100 *g*) for 15 min at 4°C. Quantitative analysis was performed on 150 μL of supernatant using an Agilent 6420B triple quadrupole (QQQ) mass spectrometer (Agilent Technologies) coupled to a 1200 series Rapid Resolution HPLC system. Details of the HPLC-MS are given in the Supplemental Dataset S1, Supplemental Materials and Methods, and Supplemental Table S3.

Transcript Quantification

Total RNA extraction was performed on the cell pellet from 10 mL of algal culture using the RNeasy Plant Mini Kit (QIAGEN). DNase treatment was carried out using TURBO DNA-free kit (Ambion), and cDNA synthesis using SuperScriptIII First-Strand synthesis system for RT-PCR (Invitrogen) according to the manufacturer's instructions. RT-qPCR was performed as described in Supplemental Dataset S1, Supplemental Materials and Methods, and Helliwell et al. (2018), using primers listed in Supplemental Table S4.

Artificial Evolution Setup

A culture of metE7 cells was plated on TAP + 1000 ng·L^{-1} B_{12} agar, and then 8 colonies picked and resuspended in TAP + 200 ng·L^{-1} B_{12} in a 96-well plate. Each well was split into 3 wells, each in a different 96-well plate containing 200 μL of a different media: TAP +1000 ng·L^{-1} B_{12}, TAP + 25 ng·L^{-1} B_{12}, and TP medium. *M. loti* was prepared in a similar manner to metE7, except preculturing was performed in TP + 0.01% (w/v) glycerol. *M. loti* was added to the TP culture containing metE7 at a density roughly 20 times greater than the alga. The 96-well plates were incubated at 25°C, under continuous light at 100 μE·m^{-2}·s^{-1}, on a shaking platform at 120 rpm. Each week the cultures were diluted: Those in TAP +1000 ng·L^{-1} B_{12} were diluted 10,000-fold, TAP + 25 ng·L^{-1} B_{12} = 100-fold, and TP = 5-fold. Every 3 weeks, 10 μL of serial dilutions of each culture was also spotted onto TAP agar + Ampicillin (50 μg·mL^{-1}) and Kasugamycin (75 μg·mL^{-1}) and TAP agar + 1000 ng·L^{-1} B_{12} to check for B_{12}-independent *C. reinhardtii*, or bacterial contaminants and to act as a reserve in the case of contamination. If cultures were found to be contaminated, then at the next transfer they were replaced by colonies from the same well that had grown on the TAP agar plates. At four points during the 12-month evolution period, all cultures were transferred to TAP agar plates where they were stored for 2 weeks during an absence from the lab, meaning that the total time in liquid culture was 10 months. See Supplemental Figure S9 for an illustration of the experimental evolution setup and the tests of B_{12} dose-response viability during B_{12} deprivation and growth in coculture with the B_{12}- producer *M. loti* that were performed on all the evolved lines.

Accession Numbers

Names and gene IDs of genes referred to in the text are given in Supplemental Table S4.

Supplemental Data

The following supplemental materials are available.

Supplemental Figure S1. Testing the B_{12} requirement of several *C. reinhardtii* strains.

Supplemental Figure S2. C1 metabolism enzyme transcript and metabolite abundances in metE7 during B_{12} deprivation and resupply.

Supplemental Figure S3. Characteristics of metE7 cells cultured in B_{12}-replete and B_{12}-deprived conditions.

Supplemental Figure S4. Composition of metE7 cells cultured in B_{12}-replete and B_{12}-deprived conditions.

Supplemental Figure S5. Amino acid and fatty acid composition of metE7 cells in B_{12}-replete and -deprived conditions.

Supplemental Figure S6. Growth and survival of metE7 under nitrogen- and B_{12}-deprivation conditions.

Supplemental Figure S7. Growth and survival of metE7 under a combination of nitrogen- and B_{12}-deprivation conditions.

Supplemental Figure S8. Growth and survival of *L. rostrata* and metE7 under B_{12}-deprivation conditions.

Supplemental Figure S9. Diagram for the experimental evolution setup and the experiments used to analyze the evolved lines.

Supplemental Figure S10. Growth parameters of the metE7 progenitor strain, and its experimental evolution descendants.

Supplemental Table S1. Information about *C. reinhardtii* strains used in this study.

Supplemental Table S2. CRISPR/Cpf1 guide RNAs and ssDNA repair templates.

Supplemental Table S3. Optimized values for Mass-spectroscopic analysis of Met cycle metabolites MRM - Positive Polarity.

Supplemental Table S4. RT-qPCR primer sequences.

Supplemental Table S5. TAP medium composition.

Supplemental Dataset S1. Quantified features of experimentally evolved lines.

Supplemental Materials and Methods. Details of the GC-MS, HPLC-MS, RT-qPCR, and statistical analyses.

Received November 8, 2019; accepted February 4, 2020; published February 20, 2020.

LITERATURE CITED

Bertrand EM, Allen AE, Dupont CL, Norden-Krichmar TM, Bai J, Valas RE, Saito MA (2012) Influence of cobalamin scarcity on diatom molecular physiology and identification of a cobalamin acquisition protein. Proc Natl Acad Sci USA **109:** E1762–E1771

Bertrand EM, Moran DM, McIlvin MR, Hoffman JM, Allen AE, Saito MA (2013) Methionine synthase interreplacement in diatom cultures and communities : Implications for the persistence of B_{12} use by eukaryotic phytoplankton. Limnol Oceanogr **58:** 1431–1450

Bertrand EM, Saito MA, Rose JM, Riesselman R, Lohan MC, Noble AE, Lee PA, DiTullio GR (2007) Vitamin B12 and iron colimitation of phytoplankton growth in the Ross Sea. Limnol Oceanogr **52:** 1079–1093

Browning TJ, Achterberg EP, Rapp I, Engel A, Bertrand EM, Tagliabue A, Moore CM (2017) Nutrient co-limitation at the boundary of an oceanic gyre. Nature **551:** 242–246

Cakmak T, Angun P, Demiray YE, Ozkan AD, Elibol Z, Tekinay T (2012) Differential effects of nitrogen and sulfur deprivation on growth and biodiesel feedstock production of *Chlamydomonas reinhardtii*. Biotechnol Bioeng **109:** 1947–1957

Chiang PK, Gordon RK, Tal J, Zeng GC, Doctor BP, Pardhasaradhi K, McCann PP (1996) S-adenosylmethionine and methylation. FASEB J **10:** 471–480

Cohen NR, Ellis K, Burns WG, Lampe RH, Schuback N, Johnson Z, Sañudo-Wilhelmy S, Marchetti A (2017) Iron and vitamin interactions in marine diatom isolates and natural assemblages of the Northeast Pacific Ocean. Limnol Oceanogr **62:** 2076–2096

Collins S, Bell G (2004) Phenotypic consequences of 1,000 generations of selection at elevated CO_2 in a green alga. Nature **431:** 566–569

Cooper MB, Kazamia E, Helliwell KE, Kudahl UJ, Sayer A, Wheeler GL, Smith AG (2019) Cross-exchange of B-vitamins underpins a mutualistic interaction between Ostreococcus tauri and *Dinoroseobacter shibae*. ISME J **13:** 334–345

Croft MT, Lawrence AD, Raux-Deery E, Warren MJ, Smith AG (2005) Algae acquire vitamin B_{12} through a symbiotic relationship with bacteria. Nature **438:** 90–93

da Silva RP, Kelly KB, Al Rajabi A, Jacobs RL (2014) Novel insights on interactions between folate and lipid metabolism. Biofactors **40:** 277–283

Davey MP, Horst I, Duong G-H, Tomsett EV, Litvinenko ACP, Howe CJ, Smith AG (2014) Triacylglyceride production and autophagous responses in *Chlamydomonas reinhardtii* depend on resource allocation and carbon source. Eukaryot Cell **13:** 392–400

Dubini A, Mus F, Seibert M, Grossman AR, Posewitz MC (2009) Flexibility in anaerobic metabolism as revealed in a mutant of *Chlamydomonas reinhardtii* lacking hydrogenase activity. J Biol Chem **284:** 7201–7213

Ducker GS, Rabinowitz JD (2017) One-carbon metabolism in health and disease. Cell Metab **25:** 27–42

Ellis KA, Cohen NR, Moreno C, Marchetti A (2017) Cobalamin-independent methionine synthase distribution and influence on vitamin B_{12} growth requirements in marine diatoms. Protist **168:** 32–47

Erickson E, Wakao S, Niyogi KK (2015) Light stress and photoprotection in *Chlamydomonas reinhardtii*. Plant J **82:** 449–465

Ferenczi A, Pyott DE, Xipnitou A, Molnar A (2017) Efficient targeted DNA editing and replacement in *Chlamydomonas reinhardtii* using Cpf1 ribonucleoproteins and single-stranded DNA. Proc Natl Acad Sci USA **114:** 13567–13572

Fu Y, Luo G-Z, Chen K, Deng X, Yu M, Han D, Hao Z, Liu J, Lu X, Dore LC, et al (2015) N6-methyldeoxyadenosine marks active transcription start sites in Chlamydomonas. Cell **161:** 879–892

Gobler C, Norman C, Panzeca C, Taylor G, Sañudo-Wilhelmy SA (2007) Effect of B-vitamins (B1, B12) and inorganic nutrients on algal bloom dynamics in a coastal ecosystem. Aquat Microb Ecol **49:** 181–194

González-Ballester D, Casero D, Cokus S, Pellegrini M, Merchant SS, Grossman AR (2010) RNA-seq analysis of sulfur-deprived Chlamydomonas cells reveals aspects of acclimation critical for cell survival. Plant Cell **22:** 2058–2084

González JC, Banerjee RV, Huang S, Sumner JS, Matthews RG (1992) Comparison of cobalamin-independent and cobalamin-dependent methionine synthases from Escherichia coli: Two solutions to the same chemical problem. Biochemistry **31:** 6045–6056

Grossman A (2000) Acclimation of *Chlamydomonas reinhardtii* to its nutrient environment. Protist **151:** 201–224

Guerra-Shinohara EM, Morita OE, Peres S, Pagliusi RA, Sampaio Neto LF, D'Almeida V, Irazusta SP, Allen RH, Stabler SP (2004) Low ratio of S-adenosylmethionine to S-adenosylhomocysteine is associated with vitamin deficiency in Brazilian pregnant women and newborns. Am J Clin Nutr **80:** 1312–1321

Heal KR, Kellogg NA, Carlson LT, Lionheart RM, Ingalls AE (2019) Metabolic consequences of cobalamin scarcity in the diatom Thalassiosira pseudonana as revealed through metabolomics. Protist **170:** 328–348

Helliwell KE (2017) The roles of B vitamins in phytoplankton nutrition: New perspectives and prospects. New Phytol **216:** 62–68

Helliwell KE, Collins S, Kazamia E, Purton S, Wheeler GL, Smith AG (2015) Fundamental shift in vitamin B_{12} eco-physiology of a model alga demonstrated by experimental evolution. ISME J **9:** 1446–1455

Helliwell KE, Pandhal J, Cooper MB, Longworth J, Kudahl UJ, Russo DA, Tomsett EV, Bunbury F, Salmon DL, Smirnoff N, et al (2018) Quantitative proteomics of a B_{12}-dependent alga grown in coculture with bacteria reveals metabolic tradeoffs required for mutualism. New Phytol **217:** 599–612

Helliwell KE, Scaife MA, Sasso S, Araujo APU, Purton S, Smith AG (2014) Unraveling vitamin B_{12}-responsive gene regulation in algae. Plant Physiol **165:** 388–397

Helliwell KE, Wheeler GL, Leptos KC, Goldstein RE, Smith AG (2011) Insights into the evolution of vitamin B_{12} auxotrophy from sequenced algal genomes. Mol Biol Evol **28:** 2921–2933

Helliwell KE, Wheeler GL, Smith AG (2013) Widespread decay of vitamin-related pathways: Coincidence or consequence? Trends Genet **29:** 469–478

Juergens MT, Deshpande RR, Lucker BF, Park J-J, Wang H, Gargouri M, Holguin FO, Disbrow B, Schaub T, Skepper JN, et al (2015) The regulation of photosynthetic structure and function during nitrogen deprivation in *Chlamydomonas reinhardtii*. Plant Physiol **167:** 558–573

Juergens MT, Disbrow B, Shachar-Hill Y (2016) The relationship of triacylglycerol and starch accumulation to carbon and energy flows during nutrient deprivation in *Chlamydomonas reinhardtii*. Plant Physiol **171:** 2445–2457

Kazamia E, Czesnick H, Nguyen TTV, Croft MT, Sherwood E, Sasso S, Hodson SJ, Warren MJ, Smith AG (2012) Mutualistic interactions between vitamin B12-dependent algae and heterotrophic bacteria exhibit regulation. Environ Microbiol **14:** 1466–1476

Kazamia E, Helliwell KE, Purton S, Smith AG (2016) How mutualisms arise in phytoplankton communities: Building eco-evolutionary principles for aquatic microbes. Ecol Lett **19:** 810–822

Kropat J, Hong-Hermesdorf A, Casero D, Ent P, Castruita M, Pellegrini M, Merchant SS, Malasarn D (2011) A revised mineral nutrient supplement increases biomass and growth rate in *Chlamydomonas reinhardtii*. Plant J **66:** 770–780

Lieber CS, Packer L (2002) S-Adenosylmethionine: Molecular, biological, and clinical aspects--an introduction. Am J Clin Nutr **76:** 1148S–1150S

Lopez D, Hamaji T, Kropat J, De Hoff P, Morselli M, Rubbi L, Fitz-Gibbon S, Gallaher SD, Merchant SS, Umen J, Pellegrini M (2015) Dynamic changes in the transcriptome and methylome of *Chlamydomonas reinhardtii* throughout its life cycle. Plant Physiol **169:** 2730–2743

Malanovic N, Streith I, Wolinski H, Rechberger G, Kohlwein SD, Tehlivets O (2008) S-adenosyl-L-homocysteine hydrolase, key enzyme of methylation metabolism, regulates phosphatidylcholine synthesis and triacylglycerol homeostasis in yeast: Implications for homocysteine as a risk factor of atherosclerosis. J Biol Chem **283:** 23989–23999

Martin NC, Goodenough UW (1975) Gametic differentiation in *Chlamydomonas reinhardtii*. I. Production of gametes and their fine structure. J Cell Biol **67:** 587–605

Meï CE, Cussac M, Haslam RP, Beaudoin F, Wong Y-S, Maréchal E, Rébeillé F (2017) C1 Metabolism inhibition and nitrogen deprivation trigger triacylglycerol accumulation in *Arabidopsis thaliana* cell cultures and highlight a role of NPC in phosphatidylcholine-to-triacylglycerol pathway. Front Plant Sci **7:** 2014

Msanne J, Xu D, Konda AR, Casas-Mollano JA, Awada T, Cahoon EB, Cerutti H (2012) Metabolic and gene expression changes triggered by nitrogen deprivation in the photoautotrophically grown microalgae *Chlamydomonas reinhardtii* and *Coccomyxa* sp. C-169. Phytochemistry **75:** 50–59

Nef C, Jung S, Mairet F, Kaas R, Grizeau D, Garnier M (2019) How haptophytes microalgae mitigate vitamin B_{12} limitation. Sci Rep **9:** 8417

Ohwada K (1973) Seasonal cycles of vitamin B_{12}, thiamine and biotin in Lake Sagami patterns of their distribution and ecological significance. Int Rev Gesamten Hydrobiol Hydrograph **58:** 851–871

Panzeca C, Beck AJ, Leblanc K, Taylor GT, Hutchins DA, Sañudo-Wilhelmy SA (2008) Potential cobalt limitation of vitamin B12 synthesis in the North Atlantic Ocean. Global Biogeochem Cyc **22:** GB2029

Panzeca C, Beck AJ, Tovar-Sanchez A, Segovia-Zavala J, Taylor GT, Gobler CJ, Sañudo-Wilhelmy SA (2009) Distributions of dissolved vitamin B12 and Co in coastal and open-ocean environments Estuarine. Coast Shelf Sc **85:** 223–230

Park JJ, Wang H, Gargouri M, Deshpande RR, Skepper JN, Holguin FO, Juergens MT, Shachar-Hill Y, Hicks LM, Gang DR (2015) The response of *Chlamydomonas reinhardtii* to nitrogen deprivation: A systems biology analysis. Plant J **81:** 611–624

Parkhill J-P, Maillet G, Cullen JJ (2001) Fluorescence-based maximal quantum yield for PSII as a diagnostic of nutrient stress. J Phycol **37:** 517–529

Provasoli L (1958) Nutrition and ecology of protozoa and algae. Annu Rev Microbiol **12:** 279–308

Ranocha P, McNeil SD, Ziemak MJ, Li C, Tarczynski MC, Hanson AD (2001) The S-methylmethionine cycle in angiosperms: Ubiquity, antiquity and activity. Plant J **25:** 575–584

Rochaix J-D (1995) *Chlamydomonas reinhardtii* as the photosynthetic yeast. Annu Rev Genet **29:** 209–230

Sañudo-Wilhelmy SA, Cutter LS, Durazo R, Smail EA, Gómez-Consarnau L, Webb EA, Prokopenko MG, Berelson WM, Karl DM (2012) Multiple B-vitamin depletion in large areas of the coastal ocean. Proc Natl Acad Sci USA **109:** 14041–14045

Sañudo-Wilhelmy SA, Gobler CJ, Okbamichael M, Taylor GT (2006) Regulation of phytoplankton dynamics by vitamin B_{12}. Geophys Res Lett **33:** L04604

Saroussi S, Karns DAJ, Thomas DC, Bloszies C, Fiehn O, Posewitz MC, Grossman AR (2019) Alternative outlets for sustaining photosynthetic electron transport during dark-to-light transitions. Proc Natl Acad Sci USA **116:** 11518–11527

Saroussi S, Sanz-Luque E, Kim RG, Grossman AR (2017) Nutrient scavenging and energy management: Acclimation responses in nitrogen and sulfur deprived Chlamydomonas. Curr Opin Plant Biol **39:** 114–122

Saroussi SI, Wittkopp TM, Grossman AR (2016) The Type II NADPH dehydrogenase facilitates cyclic electron flow, energy-dependent quenching, and

chlororespiratory metabolism during acclimation of *Chlamydomonas reinhardtii* to nitrogen deprivation. Plant Physiol **170:** 1975–1988

Sausen N, Malavasi V, Melkonian M (2018) Molecular phylogeny, systematics, and revision of the type species of Lobomonas, L. francei (Volvocales, Chlorophyta) and closely related taxa. J Phycol **54:** 198–214

Schmollinger S, Mühlhaus T, Boyle NR, Blaby IK, Casero D, Mettler T, Moseley JL, Kropat J, Sommer F, Strenkert D, et al (2014) Nitrogen-sparing mechanisms in Chlamydomonas affect the transcriptome, the proteome, and photosynthetic metabolism. Plant Cell **26:** 1410–1435

Schneider MJ, Ulland M, Sloboda RD (2008) A protein methylation pathway in *Chlamydomonas flagella* is active during flagellar resorption. Mol Biol Cell **19:** 4319–4327

Siaut M, Cuiné S, Cagnon C, Fessler B, Nguyen M, Carrier P, Beyly A, Beisson F, Triantaphylidès C, Li-Beisson Y, Peltier G (2011) Oil accumulation in the model green alga *Chlamydomonas reinhardtii*: Characterization, variability between common laboratory strains and relationship with starch reserves. BMC Biotechnol **11:** 7

Stabler SP, Allen RH, Dolce ET, Johnson MA (2006) Elevated serum S-adenosylhomocysteine in cobalamin-deficient elderly and response to treatment. Am J Clin Nutr **84:** 1422–1429

Strenkert D, Schmollinger S, Gallaher SD, Salomé PA, Purvine SO, Nicora CD, Mettler-Altmann T, Soubeyrand E, Weber APM, Lipton MS, et al (2019) Multiomics resolution of molecular events during a day in the life of Chlamydomonas. Proc Natl Acad Sci USA **116:** 2374–2383

Takeuchi T, Benning C (2019) Nitrogen-dependent coordination of cell cycle, quiescence and TAG accumulation in Chlamydomonas. Biotechnol Biofuels **12:** 292

Urzica EI, Vieler A, Hong-Hermesdorf A, Page MD, Casero D, Gallaher SD, Kropat J, Pellegrini M, Benning C, Merchant SS (2013) Remodeling of membrane lipids in iron-starved Chlamydomonas. J Biol Chem **288:** 30246–30258

Visram M, Radulovic M, Steiner S, Malanovic N, Eichmann TO, Wolinski H, Rechberger GN, Tehlivets O (2018) Homocysteine regulates fatty acid and lipid metabolism in yeast. J Biol Chem **293:** 5544–5555

Warren MJ, Raux E, Schubert HL, Escalante-Semerena JC (2002) The biosynthesis of adenosylcobalamin (vitamin B_{12}). Nat Prod Rep **19:** 390–412

White S, Anandraj A, Bux F (2011) PAM fluorometry as a tool to assess microalgal nutrient stress and monitor cellular neutral lipids. Bioresour Technol **102:** 1675–1682

Yang D, Song D, Kind T, Ma Y, Hoefkens J, Fiehn O (2015) Lipidomic analysis of *Chlamydomonas reinhardtii* under nitrogen and sulfur deprivation. PLoS One **10:** e0137948